ACS APPLIED MATERIALS & INTERFACES

Research Article

www.acsami.org

Li-Cycling Properties of Molten Salt Method Prepared Nano/Submicrometer and Micrometer-Sized CuO for Lithium Batteries

M. V. Reddy,*[,†,‡] Cai Yu,[†,§] Fan Jiahuan,[†,§] Kian Ping Loh,[‡] and B. V. R. Chowdari[†]

[†]Department of Physics, Solid State Ionics & Advanced Batteries Lab, National University of Singapore, Singapore 117542

[§]NUS High School of Mathematics and Science, 20 Clementi Avenue 1, Singapore 129957

[‡]Department of Chemistry, Graphene Research Center, National University of Singapore, Singapore 117543

Supporting Information

ABSTRACT: We report the synthesis of CuO material by molten salt method at a temperature range, 280 to 950 °C for 3 h in air. This report includes studies on the effect of morphology, crystal structure and electrochemical properties of CuO prepared at different temperatures. Obtained CuO was characterized by X-ray diffraction (XRD), scanning electron microscopy (SEM), and Brunauer–Emmett–Teller (BET) surface area methods. Samples prepared at ≥410 °C showed a single-phase material with a lattice parameter value of a = 4.69 Å, b = 3.43 Å, c = 5.13 Å and surface area values are in the range 1.0–17.0 m^2 g^{-1}. Electrochemical properties were evaluated via cyclic voltammetry (CV) and galvanostatic cycling studies. CV studies showed a minor difference in the peak potentials depending on preparation temperature and all compounds exhibit a main anodic peak at ~2.45 V and cathodic peaks at ~0.85 V and ~1.25 V vs Li. CuO prepared at 750 °C showed high and stable capacity of ~620 mA h g^{-1} at the end of 40th cycle.

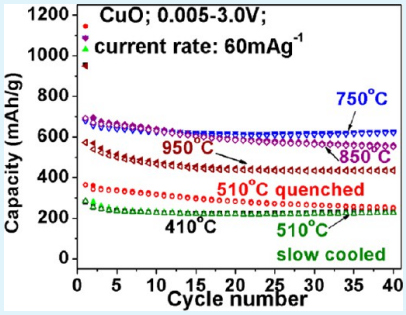

KEYWORDS: *molten salt method, CuO, $LiNO_3$:LiCl, electrochemical properties, Li-ion batteries*

INTRODUCTION

Lithium-ion batteries (LIBs) have a wide range of uses from cell phones to hybrid vehicles. The commercially used anode material for LIBs is graphite[1] which has disadvantages of poor cyclability at high current rate and low theoretical capacities of 374 mA h g^{-1} . The 3d metal oxides[1,2] (MO, M = Co, Ni, Fe, etc.) generally have high theoretical capacity and high reversible capacity and are more eco-friendly, therefore, they have been given increasing attention to serve as anode material of LIBs and as a replacement of graphite.[3−5] The electrochemical properties and conversion reaction mechanisms of binary metal oxides have been reported by Poizot et al. in the year 2000.[6] Later, Li-cycling properties of a variety of simple and complex metal oxide materials were studied by different groups.[1]

Early Li-cycling studies on CuO by the group of Tarascon,[6−8] later different CuO nanostructures were prepared by variety of chemical methods and its electrochemical properties are nicely summarized in the recent reviews.[1,2] Some of the additional recent studies have prepared CuO in the form of rods,[9] CuO/C core–shell nanowires,[10] nanocrystalline bundlelike morphology,[11] Thin film Cu_xO-TiO_2 (x = 1, 2) nanomaterials,[12] CuO nano composites,[13] CuO/Cu_2O composite in the form of mesoporous microspheres[14] and films.[15,16] However, most of the preparative methods cannot avoid the problem of tendency of capacity fading.

Molten salt synthesis is one of simple versatile method to prepare various oxides,[17−25] phosphates[26,27] and photonic crystals.[28] For academic interest presently, we report reactivity of $CuSO_4$ in 0.88M$LiNO_3$: 0.12 M LiCl molten salt in temperature range of 280–950 °C for 3 h in air and structure, morphology and its electrochemical properties. To the best of our knowledge, we are the first to report the preparation of CuO by molten salt method at various temperature and its detailed structural, morphology and electrochemical properties.

EXPERIMENTAL SECTION

Preparation of CuO. CuO powders were prepared using MSM by mixing $CuSO_4$ $5H_2O$ (Aldrich, purity 99%) and 0.88 M $LiNO_3$:0.12 M LiCl composition ($LiNO_3$: Alfa Aesar, purity 99%; LiCl: Merck, purity 99%) with a molar ratio of 1:10. Here existence of $LiNO_3$ and LiCl act as an oxidizer and mineralizing agent[29] respectively. The mixture was then heated in an alumina crucible at 280 °C for 3 h in air in a box furnace (heating and cooling rate: 3 °C min^{-1}). Afterward, the mixture was washed with distilled water to remove excess soluble Li-salts and the filtered powder was dried in an air oven at 70 °C overnight. 3–5 g of final CuO powder was obtained and stored in a desiccator for further characterization. To understand the effect of preparation temperature on formation mechanism, CuO powders were prepared at 410, 510, 750, 850, and 950 °C. Moreover, we prepared another batch at 510 °C but quenched to test whether a different way of cooling would affect electrochemical properties.

Characterization. Structural properties were determined by powder X-ray diffraction (XRD), scanning electron microscopy (SEM), and Brunauer, Emmett and Teller (BET) surface area

Received: February 14, 2013
Accepted: April 26, 2013
Published: April 26, 2013

   dx.doi.org/10.1021/am400579q | ACS Appl. Mater. Interfaces 2013, 5, 4361–4366

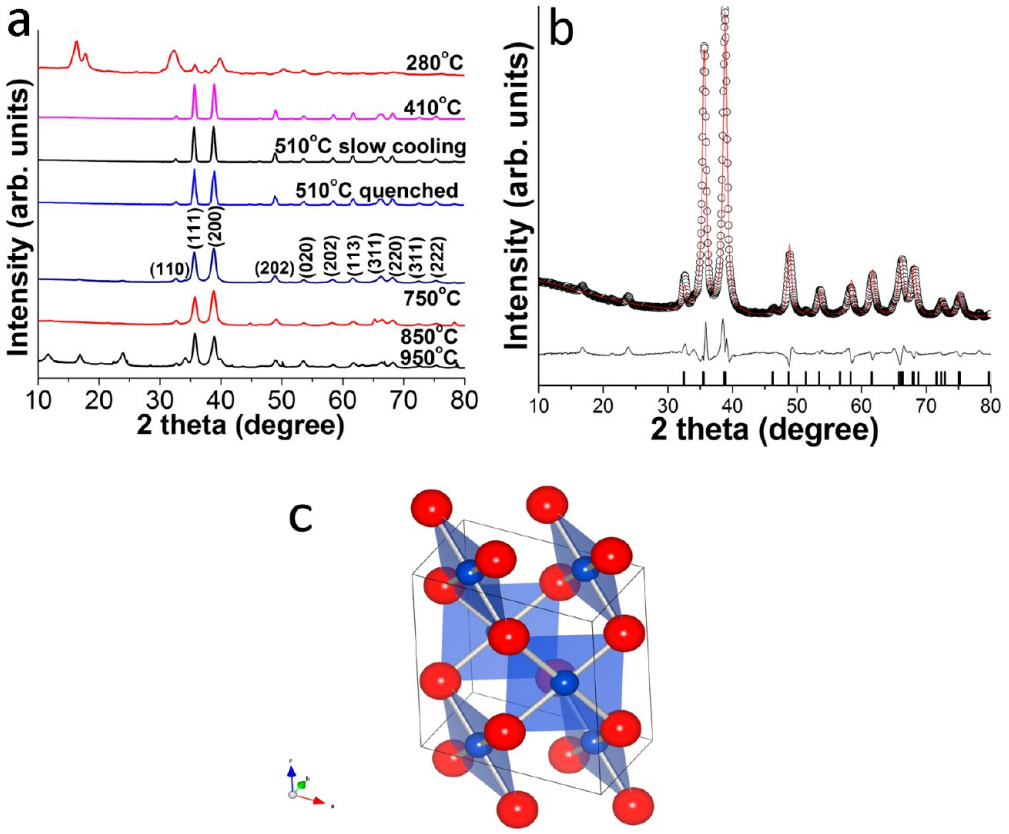

Figure 1. XRD patterns and crystal structure of CuO: (a) comparison XRD profiles of all the samples, (b) Rietveld refined XRD pattern of CuO prepared at 750 °C. The black circles correspond to observed data, the red line is the theoretical pattern, the black line is the difference between the observed data and the calculated pattern, and the vertical black bars represent the expected positions of the Bragg reflections; (c) general crystallographic representation of monoclinic CuO unit cell, red, oxygen; and pink, Cu.

method. The instrumentation details of above techniques are provided.[30] To fabricate electrodes, we mixed CuO powers as active material, super P carbon black (ENSACO, MMM Super P, 230 m^2g^{-1}), and Polymer Kynar 2801 as the binder with a weight ratio of 70:15:15. This mixture was dispersed in N-methyl pyrrolidone (NMP, Alfa Aesar) solvent to form uniform viscous slurry. The slurry was then coated on to etched copper-foil (Shenzhen Vanlead Tech. Co. Ltd., China) using doctor-blade technique and dried in an air oven at 70 °C for 12 h. The copper-foil coated with composite material was then pressed between twin rollers and cut in to circular discks with diameter of 16 mm (geometric area: 2.0 cm^2). These electrodes are dried in a vacuum oven at 70 °C for 12 h. The coin-type test cells (size 2016) were fabricated by assembling the composite electrode as anode, 1 M solution of $LiPF_6$ in ethylene carbonate (EC) and dimethyl carbonate (DMC) (1:1 by volume; Merck) as electrolyte, Whatman glass fiber paper (Aldrich) as a separator and Li-foil (diameter: 16 mm, thickness: 0.595 mm, Kyokuto metal Co. Ltd., Japan) as the counter and reference electrode. They were assembled using a coin cell crimper (Hosen, Japan) in argon-filled glovebox. The cells were tested using galvanostatic cycling and cyclic voltammetry techniques carried at room temperature 25 °C. More details on instrumentation are reported elsewhere.[23,31,32]

RESULTS AND DISCUSSION

Structure and Morphology. Prepared samples were in powder form and black in color except the sample prepared at 280 °C, which was green powder. Rietveld refinement of all the XRD patterns were fitted using TOPAS software (version 2.1). Figure 1a presents XRD patterns of all compounds and Figure.1b represents Rietveld refined XRD pattern of 750 °C sample. It shows that the experimental XRD pattern matches well with the refined data, which indicates final samples are in pure phase and absence of $LixCuO_x$ phases. The fitted lattice parameters are a = 4.693 Å, b = 3.428 Å, c = 5.13 Å. Obtained lattice parameter values are close to JCPDS card no. #89−5899 (a = 4.689(2) Å, b = 3.42(2) Å, c = 5.13(2) Å) and previous studies S. Grugeon et al[8] (a = 4.679(6) Å, b = 3.425(6) Å, c = 5.118(8) Å). Form the lattice parameter values CuO clearly shows a monoclinic structure. The (hkl) lines in the XRD patterns were generally consistent (except 280 °C prepared sample) in terms of the peak position and the height. However, we can see some minor peaks at 12, 16, and 24° (2θ) in the XRD pattern of 950 °C prepared sample. Those peaks belonged to LixCuOx phases and further careful structural studies are needed.

SEM images of CuO prepared at different temperatures are shown in Figure 2a−f. Particle sizes of obtained samples are in micrometer size range. As shown in figures, CuO prepared at 410 and 510 °C (quenched and slow cooling) (Figure 2a−c) showed irregular cauliflower-like shape, and samples prepared at 750, 850, and 950 °C showed regular needle shape, except that 950 °C sample has higher tendency to form nanowall like morphology (Figure 2d−f). BET surface area of CuO prepared at different temperature range from 0.1 to 25 m^2 g^{-1} and the pore diameter of the samples range from 13.9 to 23.2 nm (table 1).

Electrochemical Studies. Galvanostatic cycling was carried out in the voltage range, 0.005−3.0 V, and at a current rates of 60 mA g^{-1} and 600 mA g^{-1} (Figure 3). For clarity, the 1, 2, 10, 15, 20, and 25 cycles voltage vs capacity plots of CuO-750 °C at

dx.doi.org/10.1021/am400579q | ACS Appl. Mater. Interfaces 2013, 5, 4361−4366

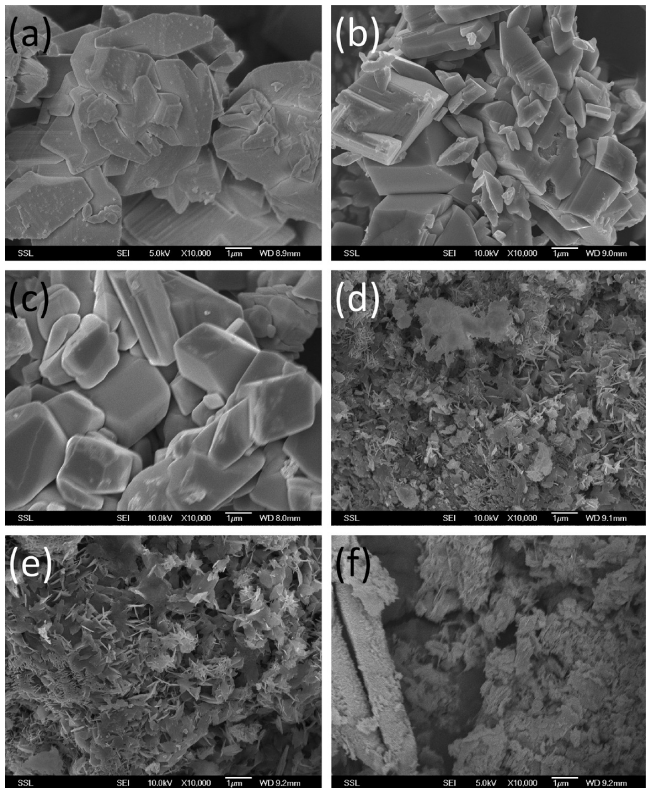

Figure 2. SEM images of CuO prepared at (a) 410 °C, 10K magnification, bar scale 1 μm; (b) 510 °C (quenched), 10K magnification, bar scale 1 μm; (c) 510 °C, 10K magnification, bar scale 1 μm; (d) 750 °C, 10K magnification, bar scale 1 μm; (e) 850 °C, 10K magnification, bar scale 1 μm; (f) 950 °C, 10K magnification, bar scale 1 μm.

a current rate of 60 mA g^{-1} are shown in Figure 3a and cycling profiles of other CuO materials prepared at different temperature are shown in Supporting Information (SI) 1. The first and second cycle plots of CuO prepared at different temperature are shown in panels b and c in Figure 3, and those with current rate of 600 mA g^{-1} are shown in panels d and e in Figure 3, respectively. The cycling profiles at low current rate (i.e., 60 mA g^{-1}) (Figure 3b) during first discharge showed a intercalation region at ∼2.20 to 1.5 V, a structure destruction/amorphization at ∼1.0 V, and a solid electrolyte interphase (SEI) at low voltage (below 0.5 V) for high temperature samples (750, 850, and 950 °C). Whereas at low temperature prepared samples (410 and 510 °C), we observed only a voltage plateau at ∼1.2 V. In subsequent discharge profiles, we observed similar features a voltage plateau ∼1.4 and ∼0.9 V. The discharge and charge capacity values are shown in Table 1.

The capacity vs cycle number plots are shown in panels a and b in Figure 4. discharge, reversible capacity and capacity fading values at current rate of 60 mA g^{-1} are given in Table 1. The irreversible capacity loss of low temperature prepared samples was ∼70% while that of samples prepared at high temperature was lower than 40%. From second cycle onward, 410 and 750 °C samples exhibits low capacity loss (less than 6%) up to 40th cycle (Table1). Comparison of capacity values of CuO-prepared at 510 °C slow cooled and quenched samples, we found out that the capacity fading of the former is much lower while the absolute reversible capacity of the latter was higher. Notably, CuO-750 °C compound showed very high and stable reversible capacity of 615 (± 5) mA h g^{-1} at the end of 20th cycle and a capacity fading of 0.76 mAh g^{-1} per cycle in the range of second-45th cycle. Our capacity retention values are better than the result previously reported by Xiang etal,[33] Mai et al.[34] and Garcia etal.[13] Mai etal[34] obtained a stable capacity of ∼500 mA h g^{-1} and a capacity fading of ∼2.5 mA h g^{-1} per cycle. A few reports of such higher- than- the theoretical capacity of CuO are: MWCNTs into leaf-like CuO nanoplates,[33] graphene-supported shuttle- and urchin-like CuO nano structures.[35] Our values are close to reported studies on CuO nanowires by Chen etal.[36] The probable reasons for the improved performance of MSM-CuO was correlated to optimum surface area, morphology and defect-free crystal structure. We do not note many comparative studies on the effect of preparation temperature on CuO, and this is first report on Li-cycling studies with various tempearatures; for academic interests, it will be nice to further study the spectroscopy and oxidation states of CuO.

Cyclic voltammetry studies were carried out with a potential range of 0.005−3.0 V vs Li/Li^+ at a scan rate of 58 mV s^{-1}. The results of cyclic voltammograms were shown in Figure 5a−e. For clarity, only selected cycles are shown and expanded graph of 410 °C, 510 °C (quenched and slow cooling) are shown as well (Figure 5a, b, d). It is clear to see the first cycle CV curves of 410 °C, 510 °C (quenched and slow cooling) compounds (Figure 5d) are of the similar shape, and first CV cycle of 750 °C, 850 and 950 °C compounds (Figure 5c, e) are in close resemblance. This result matches with the comparison we made earlier on SEM images and galvanostatic cycling results. The difference in peak intensity could due to the morphology, surface area, oxidation state, mass of the active material, and it is well-known that CV peaks currents are sensitive to mass of the active material.[37] In the first discharge cycle, common cathodic peaks are at 0.9−1.25 V for all compounds, (Figure 5), 0.7−0.85 V for 750, 850, and 950 °C (Figure 5c, e), and ∼2.0 V for 850 and 950 °C. (Figure 5e). These three main peaks correspond to a multistep electrochemical reaction (from high potential to low potential) that involves (i) reductive reaction from CuO to intercalation phase with a LixCuO-type

Table 1. Morphology, Surface Area, Discharge, Charge Capacity, and Reversible Capacity Fading (current rate, 60 mA g^{-1}) of All the Samples

CuO prepared by molten salt method at	particle size/structure	BET surface area (m^2g^{-1})	1st discharge/ (±10) $mAhg^{-1}$	1st charge/ (±5) $mAhg^{-1}$	40th charge/ (±5)$mAhg^{-1}$	Capacity fading (2−40 cyc.) %
410 °C	micrometer-sized particles	0.20 (± 0.02)	954	277	236	5.98
510 °C (slow cooling)		0.19 (± 0.02)	1031	283	227	10.63
510 °C (quenched)		0.61 (± 0.02)	1145	364	249	27.41
750 °C	submicrometer-sized particles and flakes	17.34 (± 0.1)	1090	679	619	5.64
850 °C		11 (± 0.1)	1086	692	551	17.76
950 °C		25.37 (± 0.1)	948	573	432	19.85

dx.doi.org/10.1021/am400579q | ACS Appl. Mater. Interfaces 2013, 5, 4361−4366

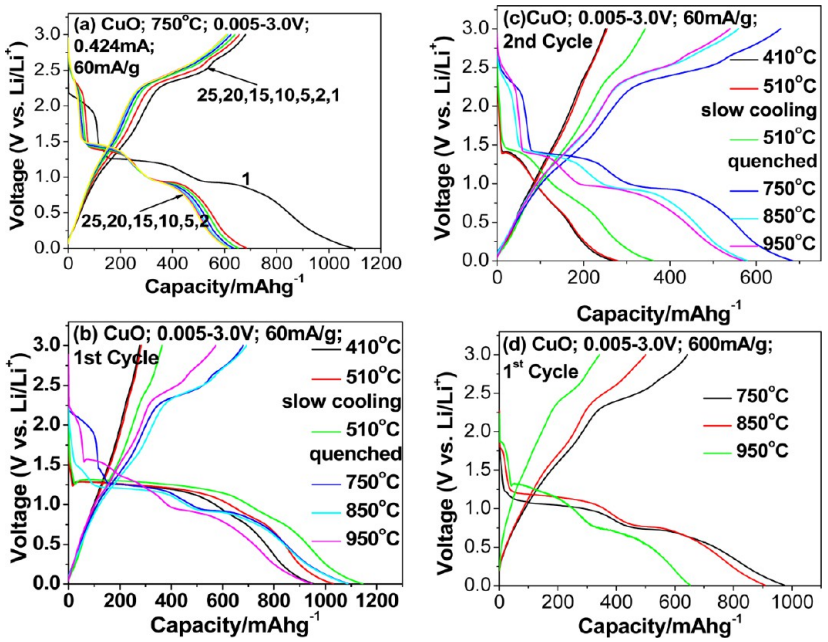

Figure 3. Galvanostatic discharge−charge cycling curves of (a) CuO-750 °C; (b) 1st cycle plot of CuO 410, 510, 510 (quenched), 750, 850, and 950 °C; (c) 2nd cycle plot of CuO 410, 510, 510 (quenched), 750, 850, and 950 °C; (d) 1st cycle plot of CuO 750, 850, and 950 °C; current rates are labeled above.

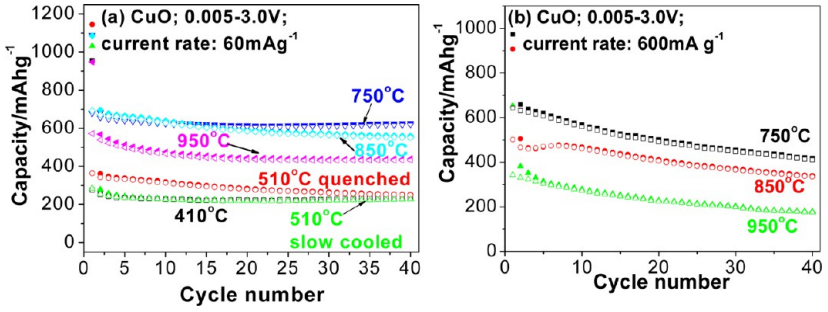

Figure 4. Discharge capacity vs cycle no. plots of (a) CuO 410, 510, 510 (quenched), 750, 850, and 950 °C at 60 mA g^{-1}; (b) CuO 750, 850, and 950 °C at 600 mA g^{-1}. Closed symbol, discharge capacity; open symbol, charge capacity.

structure; further decomposition of CuO into copper nanograins embedded into a Li_2O matrix.[7] Cathodic scan reaction can be written as $CuO+2Li+2e^- \rightarrow Li_xCuO \rightarrow Cu + Li_2O$. The extra peaks of 950 °C at 0.77 and 1.35 V (Figure 5) can be probably attributed to the destruction of extensive nanowall structure. The lack of first step reductive potential in 750 °C is due to the low starting cell voltage (∼1.9 V, whereas others are at ∼2.5 V (Figure 5). Slight differences in peak potentials are seen in CuO prepared at 410 and 510 °C (both quenched and slow cooling). Between 0 and ∼0.3 V, we can see another reductive process, and this can be attributed to the reduction of solvent in the electrolyte and hence the growth of polymeric layer. During the first charging cycle, except common anodic peak observed 0−0.5 V. Another common peak is at ∼2.43−2.53 V, and it is attributed to oxidation of Cu to CuO and most common reformation of CuO peak obtained at 2.73 to 2.80 V for the samples prepared at 750 °C, 850 and 950 °C. The charge or anodic scan reaction can be written as $Cu + Li_2O \rightarrow CuO + 2e^- + 2Li$. Second cycle and onward, we observed that all peaks of first cycles are slightly shifted to higher potential with similar shape. The diminishing peaks indicate the capacity fading showed in galvanostatic cycling earlier. As shown in panel d in Figure 5, fifth cycle of all compounds (except for fourth for 410 °C) showed a similar shape with difference in peak intensity, which can be attributed to the amount of effective compound within cells. The main cathodic and anodic peaks of 750, 850, and 950 °C fit well with the CuO and CuO/graphene prepared by hydrothermal synthesis.[34] Slight differences in peak potentials are seen due to reaction temperature, initial salt and preparation methods.

CONCLUSIONS

We have successfully synthesized nano/submicrometer size CuO composites using MSM at different temperatures. Materials were characterized by XRD, SEM and BET surface area methods. Galvanostatic cycling of CuO prepared at 750 °C at 60 mA g^{-1} in the voltage range, 0.005−3.0 V exhibits first charge capacity of 679 mA h g^{-1}. At the end of 20th cycle, it exhibits a high and stable discharge capacity of ∼615 (± 5) mA h g^{-1}. CV and galvanostatic cycling studies shows average discharge/charge reaction plateau potential was ∼0.9−1.25 V and ∼2.25−2.45 V vs Li/Li^+, respectively. For practical applications lower discharge−charge potentials are needed.

dx.doi.org/10.1021/am400579q | ACS Appl. Mater. Interfaces 2013, 5, 4361−4366

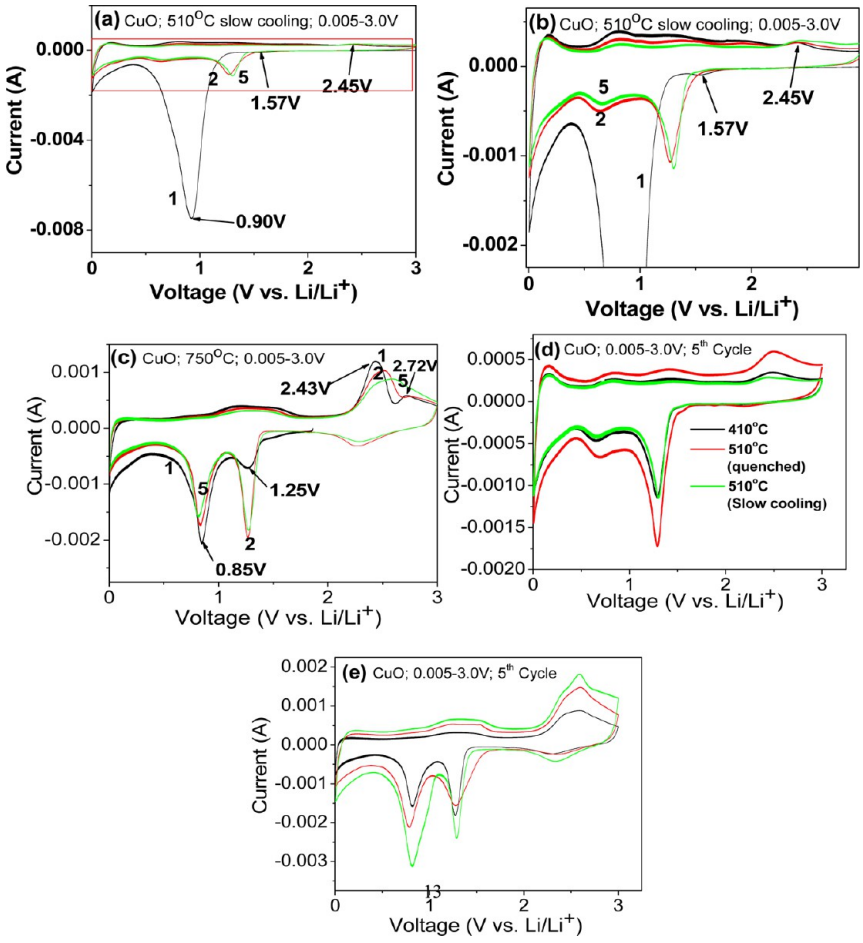

Figure 5. Cyclic voltammetry studies (a) CuO 510 °C slow cooling; (b) expanded graph CuO 510 °C slow cooling; (c) CuO 750 °C; (d) 5th cycle plot of 510 °C (both slow cooling and quenched) and 4th cycle of CuO 410 °C; (e) 5th cycle plot of 750 (black), 850 (red), and 950 °C (green), scan rate 0.058 mV s^{-1}.

■ ASSOCIATED CONTENT

Supporting Information

Voltage vs capacity plots of CuO prepared at (a) 410 °C, (b) 510 °C slow cooling, (c) 510 °C quenched, (d) 750 °C, (e, g) 850 °C, and (f, h) 950 °C, V = 0.005−3.0 V, current rate 60 and 600 mA g^{-1} . This material is available free of charge via the Internet at http://pubs.acs.org.

■ AUTHOR INFORMATION

Corresponding Author

*E-mail: phymvvr@nus.edu.sg or reddymvvr@gmail.com. Telephone number: +65-65162605; Fax: +65-67776126.

Notes

The authors declare no competing financial interest.

■ ACKNOWLEDGMENTS

The authors thank Mrs. Chong Ai Lin, Mr. Chiam Sher-Yi, Mr. See Sin Hon. and other 2011 SCIENTIA organizers from faculty of science, NUS. and NUS high school Singapore. M.V.R. thanks the National Research Foundation (NRF) Singapore for NRF-CRP Grant R-144-000-295-281 and Grant R-143-000-360-281.

■ REFERENCES

(1) Reddy, M. V.; Subba Rao, G. V.; Chowdari, B. V. R. *Chem. Rev.* **2013**, DOI/10.1021/cr3001884 (accessed 19th April 2013).
(2) Cabana, J.; Monconduit, L.; Larcher, D.; Palacin, M. R. *Adv. Mater.* **2010**, *22*, E170−E192.
(3) Magasinski, A.; Zdyrko, B.; Kovalenko, I.; Hertzberg, B.; Burtovyy, R.; Huebner, C. F.; Fuller, T. F.; Luzinov, I.; Yushin, G. *ACS Appl. Mater. Interfaces* **2010**, *2*, 3004−3010.
(4) Hertzberg, B.; Alexeev, A.; Yushin, G. *J. Am. Chem. Soc.* **2010**, *132*, 8548−8552.
(5) Reddy, A. L. M.; Gowda, S. R.; Shaijumon, M. M.; Ajayan, P. M. *Adv. Mater.* **2012**, *24*, 5045−5064.
(6) Poizot, P.; Laruelle, S.; Grugeon, S.; Dupont, L.; Tarascon, J. M. *Nature* **2000**, *407*, 496−499.
(7) Debart, A.; Dupont, L.; Poizot, P.; Leriche, J. B.; Tarascon, J. M. *J. Electrochem. Soc.* **2001**, *148*, A1266−A1274.
(8) Grugeon, S.; Laruelle, S.; Herrera-Urbina, R.; Dupont, L.; Poizot, P.; Tarascon, J. M. *J. Electrochem. Soc.* **2001**, *148*, A285−A292.
(9) Wang, L. L.; Gong, H. X.; Wang, C. H.; Wang, D. K.; Tang, K. B.; Qian, Y. T. *Nanoscale* **2012**, *4*, 6850−6855.
(10) Liu, X. Q.; Li, Z.; Zhang, Q.; Li, F.; Kong, T. *Mater. Lett.* **2012**, *80*, 37−39.
(11) Wang, L. L.; Cheng, W.; Gong, H. X.; Wang, C. H.; Wang, D.; Tang, K. B.; Qian, Y. T. *J. Mater. Chem.* **2012**, *22*, 11297−11302.
(12) Barreca, D.; Carraro, G.; Gasparotto, A.; Maccato, C.; Cruz-Yusta, M.; Gomez-Camer, J. L.; Morales, J.; Sada, C.; Sanchez, L. *ACS Appl. Mater. Interfaces* **2012**, *4*, 3610−3619.
(13) Garcia-Tamayo, E.; Valvo, M.; Lafont, U.; Locati, C.; Munao, D.; Kelder, E. M. *J. Power Sources* **2011**, *196*, 6425−6432.
(14) Zhang, Z. L.; Chen, H.; She, X. L.; Sun, J.; Teo, J.; Su, F. B. *J. Power Sources* **2012**, *217*, 336−344.

(15) Lamberti, A.; Destro, M.; Bianco, S.; Quaglio, M.; Chiodoni, A.; Pirri, C. F.; Gerbaldi, C. *Electrochim. Acta* **2012**, *86*, 323−329.
(16) Lamberti, A.; Destro, M.; Bianco, S.; Quaglio, M.; Chiodoni, A.; Pirri, C. F.; Gerbaldi, C. *Electrochim. Acta* **2012**, *70*, 62−68.
(17) Afanasiev, P.; Geantet, C. *Coord. Chem. Rev.* **1998**, *178*, 1725−1752.
(18) Kim, J. H.; Myung, S. T.; Yoon, C. S.; Kang, S. G.; Sun, Y. K. *Chem. Mater.* **2004**, *16*, 906−914.
(19) Park, H.; Yang, S. H.; Jun, Y. S.; Hong, W. H.; Kang, J. K. *Chem. Mater.* **2007**, *19*, 535−542.
(20) Zhou, H.; Mao, Y.; Wong, S. S. *Chem. Mater.* **2007**, *19*, 5238−5249.
(21) Li, L. H.; Deng, J. X.; Chen, J.; Sun, X. Y.; Yu, R. B.; Liu, G. R.; Xing, X. R. *Chem. Mater.* **2009**, *21*, 1207−1213.
(22) Reddy, M. V.; Kenrick, K. Y. H.; Wei, T. Y.; Chong, G. Y.; Leong, G. H.; Chowdari, B. V. R. *J. Electrochem. Soc.* **2011**, *158*, A1423−A1430.
(23) Reddy, M. V.; Yu, C.; Jiahuan, F.; Loh, K. P.; Chowdari, B. V. R. *RSC Advances* **2012**, *2*, 9619−9625.
(24) Zhu, P.; Reddy, M. V.; Wu, Y.; Peng, S.; Yang, S.; Nair, A. S.; Loh, K. P.; Chowdari, B. V. R.; Ramakrishna, S. *Chem. Commun.* **2012**, *48*, 10865−10867.
(25) Reddy, M. V.; Beichen, Zhang; Loh, K. P.; Chowdari, B. V. R. *CrystEngComm* **2013**, *15*, 3568−3574.
(26) Afanasiev, P. *Chem. Mater.* **1999**, *11*, 1999−2007.
(27) Huang, Q.; Hwu, S. J. *Chem. Mater.* **2001**, *13*, 1794−1799.
(28) Arpin, K. A.; Losego, M. D.; Braun, P. V. *Chem. Mater.* **2011**, *23*, 4783−4788.
(29) Reddy, M. V.; Beichen, Z.; Nicholette, L. J.; Kaimeng, Z.; Chowdari, B. V. R. *Electrochem. Solid-State Lett.* **2011**, *14*, A79−A82.
(30) Reddy, M. V.; Tung, B. D.; Yang, L.; Quang Minh, N. D.; Loh, K. P.; Chowdari, B. V. R. *J. Power Sources* **2013**, *225*, 374−381.
(31) Cherian, C. T.; Reddy, M. V.; Haur, S. C.; Chowdari, B. V. R. *ACS Appl. Mater. Interfaces* **2012**, *5*, 918−923.
(32) Christie, T. C.; Reddy, M. V.; Sow, C. H.; Chowdari, B. V. R. *RSC Advances* **2013**, *3* (9), 3118−3123.
(33) Xiang, J. Y.; Tu, J. P.; Zhang, J.; Zhong, J.; Zhang, D.; Cheng, J. P. *Electrochem. Commun.* **2010**, *12*, 1103−1107.
(34) Mai, Y. J.; Wang, X. L.; Xiang, J. Y.; Qiao, Y. Q.; Zhang, D.; Gu, C. D.; Tu, J. P. *Electrochim. Acta* **2011**, *56*, 2306−2311.
(35) Lu, L. Q.; Wang, Y. *Electrochem. Commun.* **2012**, *14*, 82−85.
(36) Chen, L. B.; Lu, N.; Xu, C. M.; Yu, H. C.; Wang, T. H. *Electrochim. Acta* **2009**, *54*, 4198−4201.
(37) Reddy, M. V.; Pecquenard, B.; Vinatier, P.; Levasseur, A. *Electrochem. Commun.* **2007**, *9*, 409−415.